Available online at www.sciencedirect.com

SciVerse ScienceDirect

Ceramics International 39 (2013) 635–640

CERAMICS INTERNATIONAL

www.elsevier.com/locate/ceramint

Al_2O_3 and ZrO_2 powders formed by centrifugal compaction using the ultra HCP method

Pawel Figiel[a,*], Lucyna Jaworska[a], Zbigniew Pedzich[b], Piotr Wyzga[a], Piotr Putyra[a], Piotr Klimczyk[a]

[a]*Centre for Materials Research and Sintering Technology, The Institute of Advanced Manufacturing Technology, Krakow 30-011, Poland*
[b]*Department of Advanced Ceramics, University of Science and Technology, Krakow 30-059, Poland*

Received 2 April 2012; received in revised form 20 June 2012; accepted 24 June 2012
Available online 29 June 2012

Abstract

The influence of high speed centrifugal compaction process, the HCP method, on the properties of green compacts and sintered samples of Al_2O_3 and ZrO_2 micropowders was investigated. This method may reduce friction between particles and prevent bridging of particles during compaction. The properties of the sintered materials strongly depend on the conditions of the centrifugal process: i.e. duration, rotation speed, solid content and dispersive liquids. The centrifugal compaction process of powder forming often results in gradient phase composition. An algorithm describing sedimentation of a group of spherical particles of different sizes and of different materials was used. Calculations for Al_2O_3 and ZrO_2 deposition for the real conditions of the high-speed centrifugal compaction process have been carried out using the Barnea–Mizrahi equation. Deposition was carried out using an ultra-centrifuge with rotational speeds of 10,000, 20,000 and 30,000 rpm for various pH of dispersive liquids. Pore size and pore size distribution of Al_2O_3 and ZrO_2 green compacts were measured by the mercury porosimetry method. Densities, Young's moduli and Vickers hardness distribution of sintered compacts prepared in various conditions are reported.

Keywords: Centrifugal compaction; Ultra HCP method; Al_2O_3 and ZrO_2 powders

1. Introduction

The gravity casting or dry processes, such as dry pressing and isostatic cold pressing, are used very often as the compacting methods of ceramic powders. Friction forces and stresses in the green compacts, however, accompany these methods and their reliability is limited by defects due to agglomerates [1]. The compacting pressure may deform and fracture the powder particles [2]. New techniques include hot isostatic pressing, aqueous injection molding, direct coagulation casting, electrophoretic forming, gelcasting, hydrolysis assisted solidification, pressure filtration, temperature induced forming. These methods have both advantages and disadvantages, and only few have been commercialized.

When powders are dispersed in slurries, friction between particles is reduced and dense and homogenous packing is attained. In the high speed centrifugal compaction process HCP, the particles sediment under a centrifugal force. Sedimentation in the HCP process depends on size, shape and density of particles, the type of dispersant, centrifuge speed, acceleration and deceleration and duration of the process. With a high compacting velocity, duration of compacting is short. Use of the HCP method results in low contamination [3], provides dense and homogenous green bodies and sintered compacts with few defects, because defects are less likely to occur under the strong centrifugal force [4].

Tashima et al. [5] prepared high purity alumina using the HCP method and obtained a ceramic characterized by very high bend strength of 1330 MPa. A drawback of this process is mass or phase segregation during consolidation, which can be eliminated by starting with highly concentrated slurry [6]. Al_2O_3 compacts manufactured using a

*Corresponding author. Tel.: +48 12 63 17 411; fax: +48 12 633 94 90.
E-mail address: pawel.figiel@ios.krakow.pl (P. Figiel).

0272-8842/$36.00
http://dx.doi.org/10.1016/j.ceramint.2012.06.075

low rotational speed are characterized [1] by low density, with a gradient, which can be eliminated by means of a sufficiently high centrifugal force [3]. To model the HCP process, we start with a single heavy spherical particle falling in a viscous fluid under the gravitational field. Stoke's settling velocity [7] is:

$$U_s = \frac{d^2(\rho-\rho_c)}{18\eta} g_0, \quad (1)$$

where d denotes the diameter of the sphere, ρ and ρ_c the densities of the particles and of the fluid, η the dynamic viscosity of the fluid and $g_0$the gravitational acceleration. Formula (1) is valid for laminar flow, when the Reynolds number $\mathrm{Re} = (U_s \rho d/\eta)$ satisfies the inequality $10^{-4} < \mathrm{Re} < 2$.

For slowly sedimenting particles, long ranged hydrodynamic interactions lead to a modification of Stocke's settling velocity.

Jones and Kutteh applied Stokesian simulations to compare the hydrodynamic interactions between colloidal particles in a fluid and near a hard wall [7], finding a high degree of symmetry in the configuration of the particles in a fluid which is broken by the presence of the walls. A similar method, based on statistical mechanics, was used to study random clouds of particles [8]. The gravitational settling of small particles was numerically investigated by Bosse et al. [9] and Lattice-Boltzmann's simulation was performed on monodispersive and polydispersive suspensions. It was verified that particle velocity fluctuations were suppressed by a no-slip condition on the walls [10]. Kynch's cinematic sedimentation model applied to high concentration suspensions and its generalizations are described in Ref. [10] and a review of recent experimental and theoretical work appeared in Ref. [11].

Taking into account hydrodynamic interactions of particles and the effect of walls, it is possible to modify formula (1), e.g. using the Barnea–Mizrahi's [12] correction:

$$U = U_s \frac{(1-\phi)^2}{(1+\phi^{1/3})\exp[5\phi/3(1-\phi)]} \quad (2)$$

where ϕ denotes concentration.

Dilute suspensions, when ϕ is small, are sufficiently well described by Eq. (2), which does not apply to higher concentrations. In the present paper, we consider the case $\phi = 0.1$, hence formula (2) can be assumed as the benchmark of our calculations. In these the gravitational acceleration g_0 is replaced by the centrifugal acceleration g which exceeds g_0 at least five times. Moreover, as the centrifugal acceleration depends on time t, the constant g_0 is replaced by the function $g(t) = r(t)\omega^2(t)$, where $r(t)$ is the distance which a particle passes from the top of the vessel to the bottom at time t and $\omega(t)$ is the angular velocity [13].

2. Experimental procedure

The starting materials were Alcoa A16SG Al_2O_3 powder (mean particles size 0.7 μm, specific surface area 8.9 m^2/g, shape factor $\beta = 1.42$, with addition of 0.3 mass% of MgO) and Tosoh Corporation ZrO_2 powder TZ-3Y (with mean particle size of 0.2 μm, specific surface area 16 m^2/g, shape factor $\beta = 1{,}2$).

Powders were dispersed in an ion-exchanged water of which pH was changed by citric acid and calcined soda. Slurries were prepared using an ultrasonic disintegrator Techpan UD-20, Nanosizer (Model ZS, Malvern Instruments), while zeta potential was measured with laser Doppler Electrophoresis. The viscosities of the slurries were measured by Höppler's viscometer.

Studies were carried out for rotational speeds from 10,000 up to 30,000 rpm, using a Model UP67 M ultracentrifuge. The distance between the centre of rotation and the top of the vessel is denoted by $r_{\min}$ and fixed at 4.0 cm. The distance to the bottom $r_{\max}$ is equal 12.88 cm, so the height of the vessel is 7.38 cm. The axis of rotation is perpendicular to the axis of the tube with 1.0 cm diameter.

Pores size and pore size distribution of green compacts were measured by the mercury porosimetry method (Model Nova 1200e, Quantachrome Instruments). Particle size distribution was measured with Shimadzu's apparatus, grain size fractions were used for calculations.

The rotational speeds of the ultra-centrifuge were 10,000, 20,000 and 30,000 rpm, for 15 min for various pH of dispersive liquids. Spherical particles are uniformly distributed in the vessel, hence we have at the initial time $t = 0$ an uniform suspension. At the beginning of the experiment the gravitational forces act upon the particles, but do not essentially change their positions. In the process of accelerated rotation, the centrifugal forces exceed the gravitational forces more than five times. This implies that the particles fall from the top to the bottom of the vessel and the gravitational effects can be neglected. An example of the dependence of angular velocity ω on the time t for 15,000 rpm is presented in Fig. 1. This dependence changes and was measured for every angular velocity.

Al_2O_3 and ZrO_2 green compacts were first dried at room temperature and next at 225 °C for 48 h (with heating rate 30 °C/h). For comparison, Al_2O_3 and ZrO_2 samples were

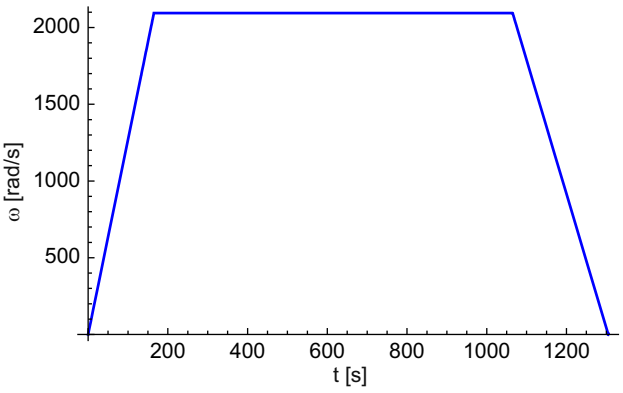

Fig. 1. Dependence of angular velocity ω on time t. Constant angular velocity is 15,000 rpm.

also prepared by uniaxial dry pressing in a steel die at 50 MPa, followed by isostatic pressing at 300 MPa.

Al_2O_2 specimens were sintered in a Nabertherm HT 16/18 furnace, with heating rate of 5 °C/min at 1650 °C for 1 h; for ZrO_2 heating rate was 2 °C/min, material was sintering at 1230 °C for 2 h. Samples for microstructural analysis, Vickers hardness measurements and Young's moduli measurements were prepared by lapping and polishing the compacts. Microstructural observations were performed using a JEOL JSM-6460LV scanning electron microscope. Density was measured using the Archimedes method. Vickers hardness was measured using FM-7 apparatus (Future Tech) at 4.9 N load. Young's modulus was measured using the ultrasonic method with EPOCH-3 (made by Panametrix) apparatus.

3. Results and discussion

A typical plot of angular velocity ω versus time t ($\omega(t)$) for deposition of Al_2O_3 and ZrO_2 particles is given in Fig. 1. The times of deposition of Al_2O_3 and ZrO_2 particles of various sizes were calculated, using the Barnea–Mizrahi's formula, and are presented in Fig. 2a and b. The calculations are only approximations because, during the process, there are a lot of variables [10]. For this narrow particle size distribution and high velocity of deposition (15,000 rpm), differences in duration of particle deposition are visible and are presented in Fig. 2a and b. The duration of centrifugal compaction depends on density, size of particles and centrifuge conditions. The deposition of the smallest particles is not possible for a too small a rotational velocity.

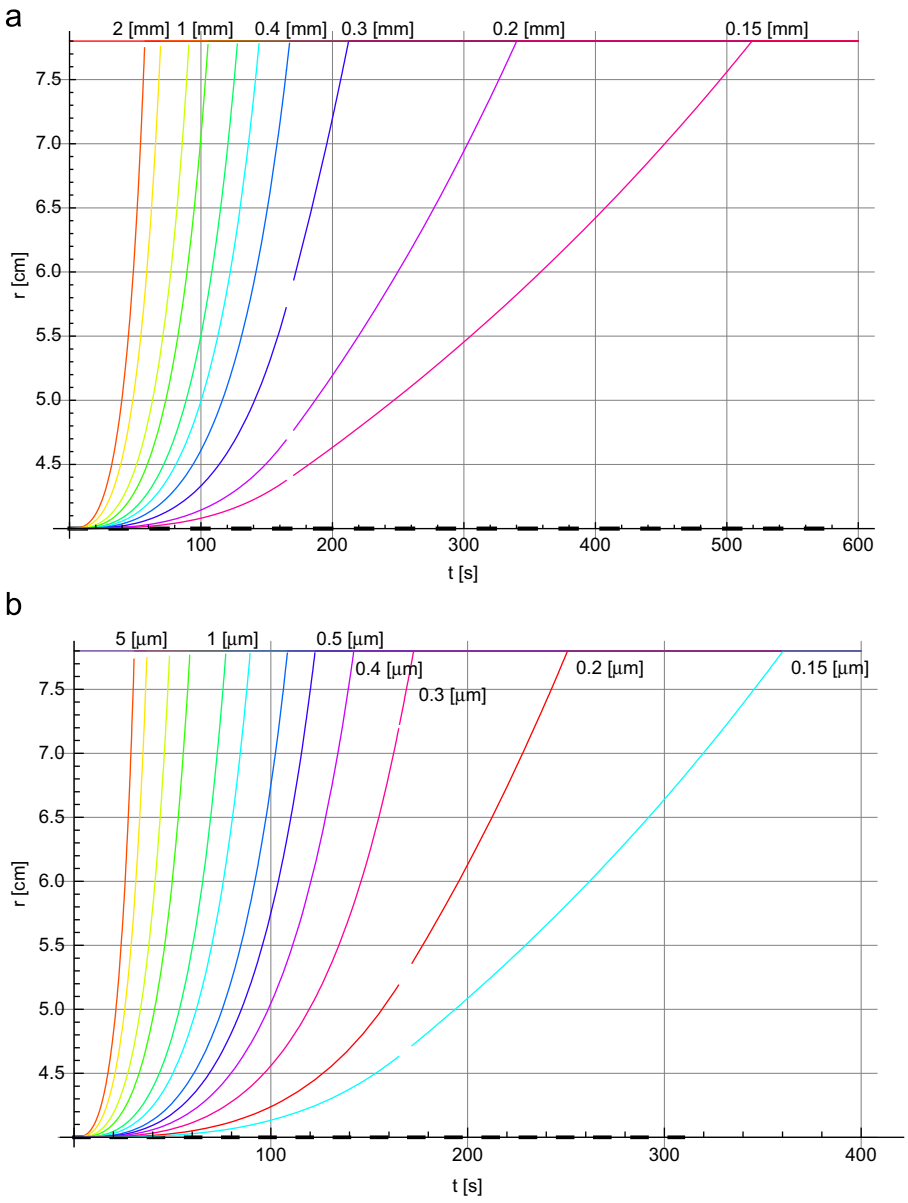

Fig. 2. $r(t)$ calculated for various diameters of particles, d (µm) for Al_2O_3 (a) and ZrO_2 (b) powders and angular velocity 20,000 rpm.

The pH of the dispersing agent is one of the most important factors in aqueous media that affects its zeta potential. The plot of zeta potential versus pH for Al_2O_3 and ZrO_2 colloidal suspensions is shown in Fig. 3. Zeta potential refers to the electrostatic potential generated by the accumulation of ions at the surface of a colloidal particle. It helps to maximize the repulsive forces between them in order to keep each particle discrete and prevents them from gathering into larger, faster settling agglomerates. The isoelectric point for these colloidal suspensions for Al_2O_3 is approximately pH 9 and for ZrO_2 pH 8.8. For pH close to the isoelectric point there are problems with the coagulation and forming of an aggregate.

Studies of pores distribution were conducted for various pH in the range 2.8–9.55. The influence of pH of the aqueous medium on the pore size and pore distributions in Al_2O_3 green compacts produced by HCP (15,000 rpm, 15 min) and, for comparison, by axial pressing of the same powder at 300 MPa are presented in Fig. 4. Samples compacted at high pH are characterized by small sizes of pores, but their amount is higher than for the samples compacted at low pH values. The sample pressed at 300 MPa is characterized by a high presence of small pores.

The most representative parameter in porosimetry studies of green compacts is the cumulative pore volume per mass unit. The best result for ZrO_2 compacted at 15,000 rpm for 15 min was achieved for pH 4.7. For axially pressed samples the sizes of pores are about 30 nm. The results for ZrO_2 green compacts obtained from colloidal aqueous suspensions for pH 2.0, 4.7 and 9.15 and for samples pressed at 50 and 300 MPa are presented in Fig. 5.

Using the results of the pore size distribution, pH 4.7 was chosen for the studies of ZrO_2 slurries. For this condition pore size and pore distribution are similar to the samples pressed at 300 MPa. In Fig. 6a and b are presented density measurements for sintered Al_2O_3 compacts, formed by HCP at 10,000 rpm and 30,000 rpm during 7, 15, 20 min, and for sintered compacts pressed at 300 MPa,

The results are very similar; sintered densities of HCP samples were higher than of the sample pressed at 300 MPa. There is no strong influence of the centrifugal speed on compacts' densities. The best results are obtained for 15 min's time of centrifugation. Young's modulus measurements are shown in Fig. 7, the tendency is the same as for densities (Fig. 6).

The hardness of Al_2O_3 compacts prepared using HCP method at 30,000 rpm and of a pressed sample is presented in Fig. 8. The hardness, for both fabrication methods, was inhomogeneous and varied with the sample height. The highest average values of hardness were for a sample obtained by HCP at 30,000 rpm during 15 min.

Results of density and hardness of ZrO_2 compacts are shown in Figs. 9 and 10. ZrO_2 compacts formed by HCP are characterized by different types of microstructure at the top and at the bottom of the sample, Fig. 11a–c. At the bottom, no visible porosity can be observed and the average size of the ZrO_2 particles is 0.5 μm, Fig. 11a and b. This part of the samples is composed of larger particles, which are not

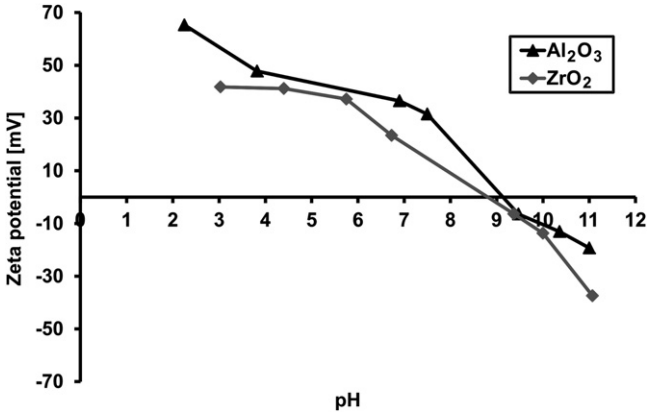

Fig. 3. Zeta potential versus pH for Al_2O_3 and ZrO_2 particles deposited in an aqueous medium.

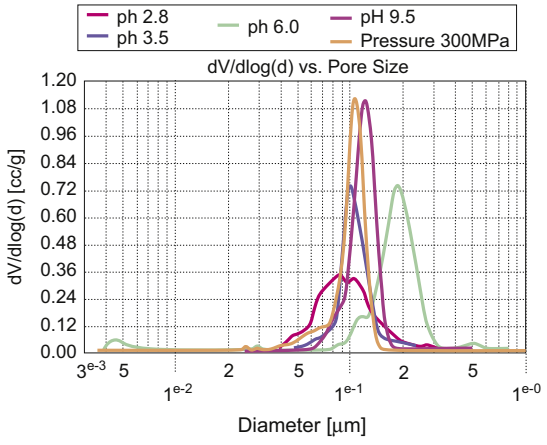

Fig. 4. Pore size distribution for Al_2O_3 green compacts obtained from colloidal aqueous suspensions at pH 2.8, 3.54, 6.07, and 9.55, centrifuged at 15,000 rpm for 15 min and for samples uniaxially pressed at 300 MPa.

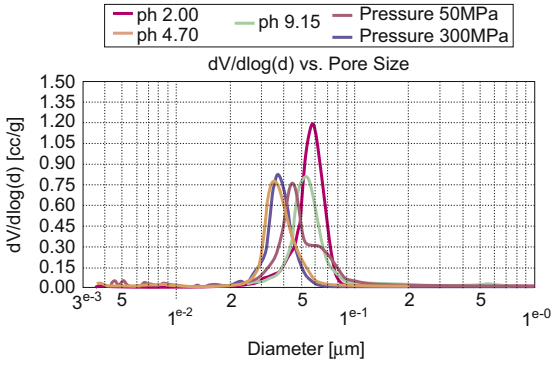

Fig. 5. Pore size distribution for ZrO_2 green compacts obtained from colloidal aqueous suspensions at pH 2.0, 4.7 and 9.15 centrifuged at 15,000 rpm for 15 min and for samples uniaxially pressed at 50 and 300 MPa, respectively.

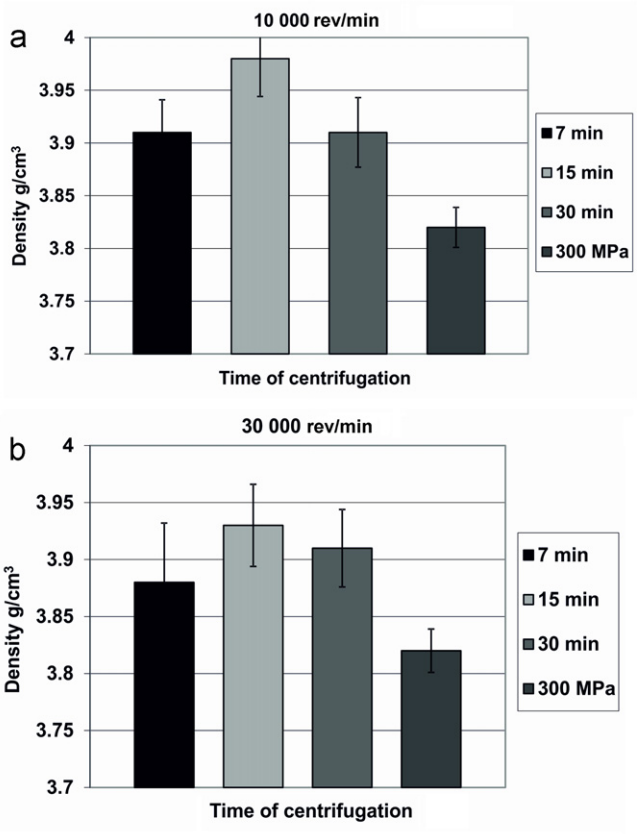

Fig. 6. Densities for sintered Al_2O_3 compacts formed by HCP at 10,000 rpm (a) and 30,000 rpm (b) during 7, 15 and 30 min and for sintered compacts pressed at 300 MPa.

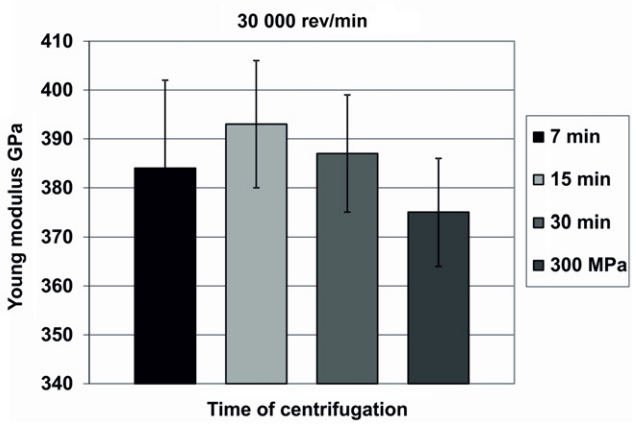

Fig. 7. Young's moduli for sintered Al_2O_3 compacts, formed by HCP at 30,000 rpm during 7, 15 and 30 min and for sintered compacts pressed at 300 MPa.

porous and are transparent. The average size of particles at the top part of the sample is 0.34 μm and pores are visible.

4. Conclusions

(1) The reliability of a dry pressed ceramic is limited by defects due to agglomerates and internal stresses. Most colloidal forming techniques are limited due to the density gradient in the green compact. Wet processing routes provide a possibility of breaking down agglomerates, but they create differential sedimentation due to particle size distribution.

(2) In this work, water was used as a dispersive agent. The use of water is the highest attribute of colloidal processes—from the environmental point of view.

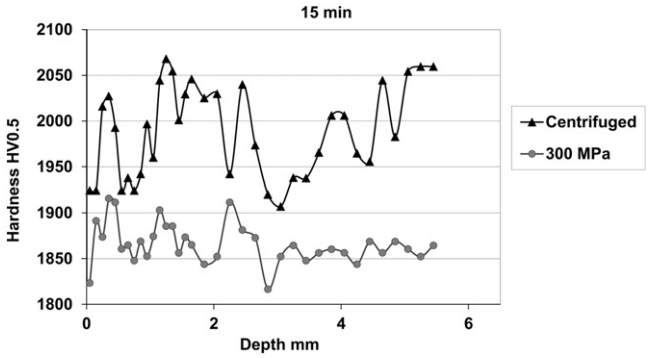

Fig. 8. Hardness of Al_2O_3 compacts prepared by HCP method at 10,000, 20,000 and 30,000 rpm during 15 min (cross-section from the top to the bottom of the sample) and for a pressed sample.

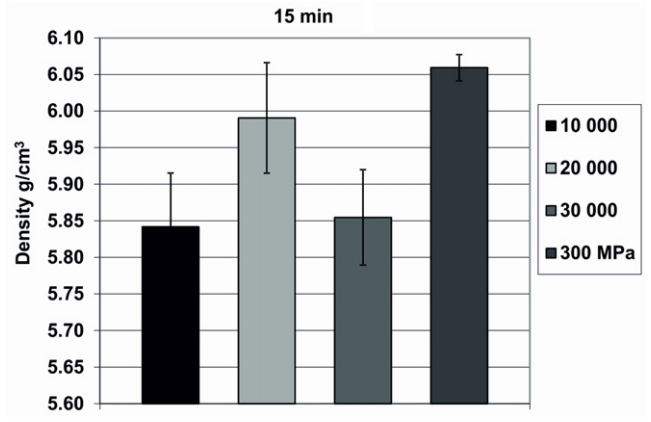

Fig. 9. Densities for sintered ZrO_2 compacts formed using HCP at 10,000, 20,000 and 30,000 rpm during 15 min and for sintered compacts pressed at 300 MPa.

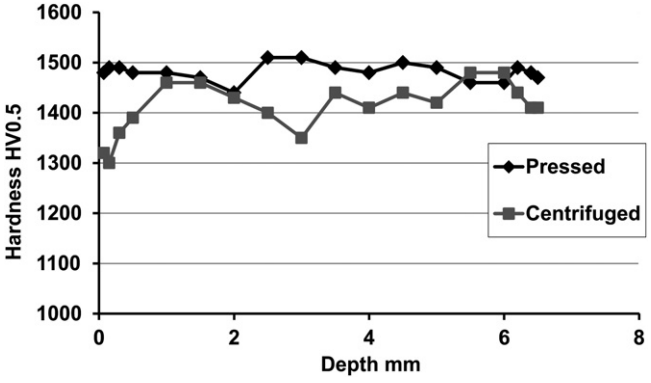

Fig. 10. Hardness of the ZrO_2 compacts prepared by the HCP method at 30,000 rpm during 15 min (from the top to the bottom of samples) and for a pressed sample.

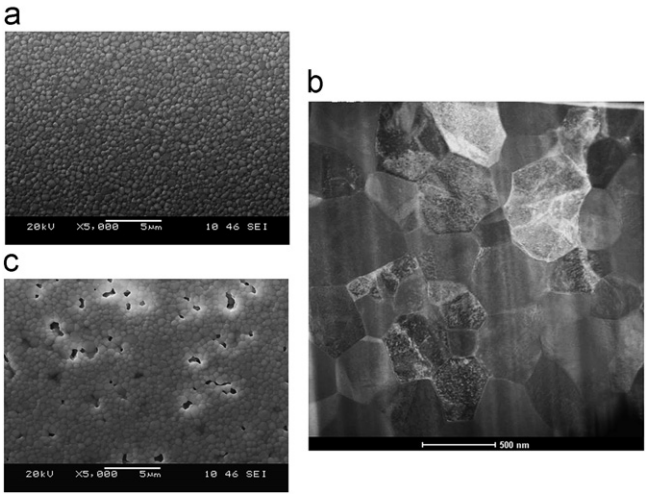

Fig. 11. Microstructures of HCP formed ZrO_2 sample; (a) top part, (b) and (c) bottom part of the sample.

(3) Measurements confirm that the velocity of the compaction process has an influence on duration of particles' deposition. It is possible to reduce the duration of compaction by increasing the centrifugal speed.
(4) The duration of deposition of Al_2O_3 and ZrO_2 particles of various sizes was calculated using the Barnea–Mizrahi's formula. From these calculations, for a narrow particles size distribution and high velocity of deposition, there are differences in durations of compacting. Time of centrifugal compaction depends on density, size of particles and centrifuge conditions. For a too small a rotary velocity, the smallest particles could not be deposited.
(5) Properties of green and sintered compacts, apart from the significant influence of duration of deposition, rotational speed, solid content, dispersion liquid, are also influenced by pH of the dispersing agent. The pH of the aqueous medium affects its zeta potential. For Al_2O_3 slurries the lowest cumulative pore value of 196.5 mm^2/g is for 3.95 pH. For ZrO_2 slurries, for153.1 mm^3/g, it is for pH 4.7. Porosity and the pore distribution strongly depend on pH of the colloidal aqueous suspensions.
(6) The pore sizes and distributions for green compacts after centrifugal casting and after uniaxial pressing at 300 MPa are similar. Pore size distribution for ZrO_2 centrifugal compaction is comparable to that in samples pressed at 300 MPa, but the latter are characterized by lower values of densities and hardness.
(7) A limitation of the HCP method is a gradient of particles sizes. For a monolithic material, the solution for prevention of this defect is a narrow fraction of particles sizes.
(8) Density, hardness and Young's modulus of the Al_2O_3 compact, obtained by the HCP method are better than for the pressed samples.

References

[1] H.Y. Suzuki, K. Shinozaki, S. Tashima, H. Kuroki, Effect of High Centrifugal Force on Properties of Green Compacts Made by High-Speed Centrifugal Compaction Process, in: K. Kosuge, H. Nagai (Eds.), 2000 Powder Metallurgy Congress Proceedings, Japan Society of Powder Metallurgy, Vol. 1, Japan Powder Metallurgy Association, Kyoto, 2000, pp. 582–585.
[2] Z.S. Rak, Advanced Forming Techniques in Ceramics, in: J. Lis (Ed.), Polish Ceramics 2000 Conference Proceedings, Polish Ceramic Society, Spala, 2000, pp. 1–18.
[3] H.Y. Suzuki, S. Tashima, Hidenori K., Homogeneous Compaction of Fine Ceramic and Carbide Powders by High Speed Centrifugal Compaction Process, Euro PM 2002 Proceedings - Hard Materials Proceedings, European Powder Metallurgy Association, Shrewsbury, 2002, pp. 46–51.
[4] K. Sato, Y. Hotta, H. Yilmaz, K. Watari, Fabrication of green and sintered bodies prepared by centrifugal compaction using wet-jet milled slurries,, Journal of the European Ceramic Society 29 (2009) 1323–1329.
[5] S. Tashima, M. Sumita, H. Kuroki, Centrifugal compaction of submicron high purity alumina powder, Japan Society of Powder and Powder Metallurgy 39 (1992) 39–43.
[6] P. Rao, M. Iwasa, T. Tanaka, I. Kondoh, Centrifugal casting of Al_2O_3-15 wt% ZrO2 ceramic composites, Ceramic International 29 (2003) 20–212.
[7] R.B. Jones, R. Kutteh, Sedimentation of colloidal particles near a wall: Stokesian dynamic simulations, Physical Chemistry Chemical Physics 1 (1999) 2121–2139.
[8] M.L. Ekel-Jeżewska, B. Metzger, E. Guazzelli, Spherical cloud of point particles falling in a viscous fluid, Physics of Fluids 18 (2006) 038104.
[9] T. Bosse, L. Kleiser, E. Meiburg, Small particles in homogeneous turbulence: Settling velocity enhancement by two-way coupling, Physics of Fluids 18 (2006) 027102.
[10] M.C. Bustos, R. Burger, F. Concha, E.M. Tory, Sedimentation and Thickening, Fourth ed., Kluwer Academic Publ, Dordrecht, 1999.
[11] S. Ramaswamy, Issues in the statistical mechanics of steady sedimentation, Advances in Physics 50/3 (2001) 297–341.
[12] V. Mityushev, L. Jaworska, M. Rozmus, B. Krolicka, Compaction of the diamond – Ti_3SiC_2 graded material by the high speed centrifugal compaction process, Archives of Materials Science and Engineering 28/11 (2007) 677–682.
[13] L. Jaworska, V. Mitiuszew, Z. Pędzich, L. Stobierski, M. Rozmus, P. Figiel, Centrifugal compaction of submicro- and nanopowders, Ceramika 103/2 (2008) 812–2008.